



Room temperature long-lived triplet excited state of fluorescein in $N^{\wedge}N$ Pt(II) bisacetylide complex and its applications for triplet–triplet annihilation based upconversions

Wenting Wu, Jianzhang Zhao*, Wanhua Wu, Yinghui Chen

State Key Laboratory of Fine Chemicals, School of Chemical Engineering, Dalian University of Technology, E-208 Western Campus, 2 Ling-Gong Road, Dalian 116024, China¹

ARTICLE INFO

Article history:

Received 21 March 2012

Received in revised form

11 May 2012

Accepted 15 May 2012

Keywords:

Photochemistry

Fluorescein

Platinum

Upconversions

DFT

Triplet state

ABSTRACT

The room temperature (RT) long-lived triplet excited state of fluorescein was observed in a *dbbpy* Pt(II) bisfluorescein acetylide complex (**Pt-1**, where *dbbpy* = 4,4'-di(*tert*-butyl)-2,2'-bipyridine). The complex shows strong absorption of visible light ($\epsilon = 24,600 \text{ M}^{-1} \text{ cm}^{-1}$ at 457 nm). Interestingly, the phosphorescence of the coordination centre is completely quenched and only the fluorescence of ligand was observed for **Pt-1** at RT. At 77 K, a phosphorescence band at 667 nm was observed. Spin density analysis and nanosecond time-resolved transient difference absorption spectroscopy proved that the lowest-lying triplet excited state of the complex **Pt-1** is localized on the fluorescein acetylide ligand (^3IL state), for which the lifetime was determined as 16.4 μs (RT, by the time-resolved transient absorption spectra). The quenching of the $^3\text{MLCT}$ phosphorescence in **Pt-1** is due to the intramolecular energy transfer of $^3\text{MLCT} \rightarrow ^3\text{IL}$. The complex **Pt-1** was used as the triplet sensitizer for the triplet–triplet annihilation (TTA) based upconversion. Our results will be useful for preparation of transition metal complexes that show intense absorption of visible light and long-lived triplet excited states, these photophysical properties are useful for applications in photovoltaics, photocatalysis or upconversions, etc.

© 2012 Elsevier B.V. All rights reserved.

1. Introduction

Fluorescein has attracted much attention due to its fluorescence properties, and has been extensively used in fluorescent molecular probes [1–4]. However, in stark contrast to the studies of its fluorescence (i.e. radiative $S_1 \rightarrow S_0$ transition), the phosphorescence or the triplet excited state of fluorescein has never been explored. Different from the manifold of singlet excited states, chromophores with triplet excited states populated upon photoexcitation are crucial for applications such as photodynamic therapy (PDT) [5], photocatalysis [6], and more recently the triplet–triplet annihilation (TTA) based upconversions [7–20]. However, it is not easy to access the triplet excited states of the organic chromophores, usually heavy atom effect is required for the inter-system crossing (ISC) [21,22].

On the other hand, phosphorescent transition metal complexes usually show efficient ISC, by which the triplet excited state is produced [21,23–26]. For example, $N^{\wedge}N$ Pt(II) bisacetylide are representative for their room temperature (RT) phosphorescence

(where $N^{\wedge}N$ is bidentate ligand, such as *dbbpy* = 4,4'-di(*tert*-butyl)-2,2'-bipyridine) [23,27]. The heavy atom effect of Pt(II) facilitates the ISC, thus the fluorescence ($S_1 \rightarrow S_0$) of the acetylide ligands is quenched. Previously perylene diimide acetylide has been attached to Pt(II) centre [28], but no phosphorescence has been observed, which is in contrast to the model complex *dbbpy* Pt(II) bisphenylacetylide gives emission at 560 nm ($\Phi = 51\%$, $\tau = 1.36 \mu\text{s}$) [27,29]. However, usually transition metal complexes show weak absorption in the visible region [23]. For example, *dbbpy* Pt(II) bisphenylacetylide shows $\epsilon = 9300 \text{ M}^{-1} \text{ cm}^{-1}$ at 397 nm [23,27,28]. Furthermore, the lifetime of the T_1 excited state of these complexes are usually less than 5.0 μs [23,30]. Complexes with strong absorption of visible light and long-lived triplet excited state are useful for applications such as photocatalysis [6], photovoltaics [31,32], and TTA upconversions, etc [8–20].

Recently we proposed a straight forward approach to prepare transition metal complexes that show intense absorption of visible light and long-lived triplet excited states, that is, to attach organic chromophore to the Pt(II) centre via acetylide bonds [16,17,33]. With this approach, chromophores of naphthalimide (NI) [33], coumarin [16], naphthalenediimide (NDI) [17], and rhodamine have been attached to the Pt(II) centre [20]. Based on the photophysical properties of these complexes, we found that direct attachment of

* Corresponding author. Tel./fax: +86 (0) 411 8498 6236.

E-mail address: zhaojzh@dlut.edu.cn (J. Zhao).

¹ <http://finechem.dlut.edu.cn/photochem>.

the π -core of organic chromophore to the metal centre usually gives RT phosphorescence of the organic chromophore [17,33]. Conversely, for those complexes with the organic chromophore *dangled* at the peripheral moiety (not the π -core) of the coordination centre, no RT phosphorescence of the ligand was observed, instead, the fluorescence of ligand was observed [20]. However, we also proved that even *without* the RT phosphorescence, the transient metal complexes are still useful for applications such as TTA based upconversions, given that the non-emissive intraligand triplet excited state (^3IL) was populated upon photoexcitation of the complex [20]. The lifetime of the triplet excited state of these organic chromophore-containing Pt(II) complexes are usually long. For example, T_1 state lifetime up to 83.0 μs was observed with rhodamine attached to the Pt(II) centre [20].

In order to study the RT triplet excited state of fluorescein, herein we devised a fluorescein-containing Pt(II) acetylide complex **Pt-1** (Scheme 1). Model complex **Pt-2** with phenylacetylide ligands was used in the photophysical studies. **Pt-1** shows intense absorption of visible light ($\epsilon = 24,600 \text{ M}^{-1} \text{ cm}^{-1}$ at 457 nm). Interestingly, only fluorescence of the fluorescein ligand was observed for **Pt-1** at RT. Nanosecond time-resolved transient absorption spectra and spin density analysis proved that the ^3IL state localized on the fluorescein moiety was populated. Phosphorescence of the fluorescein ligand was observed for **Pt-1** at 77 K. **Pt-1** was used as efficient triplet sensitizer for TTA upconversion and upconversion quantum yield of 10.7% was observed.

2. Results and discussion

2.1. Design and synthesis of the complexes

In order to exclude the undesired effect of the lactum/lactone structure of the fluorescein on the photophysics of the complex **Pt-1** (Scheme 1) [3,4], we used an acetylide ligand that without the

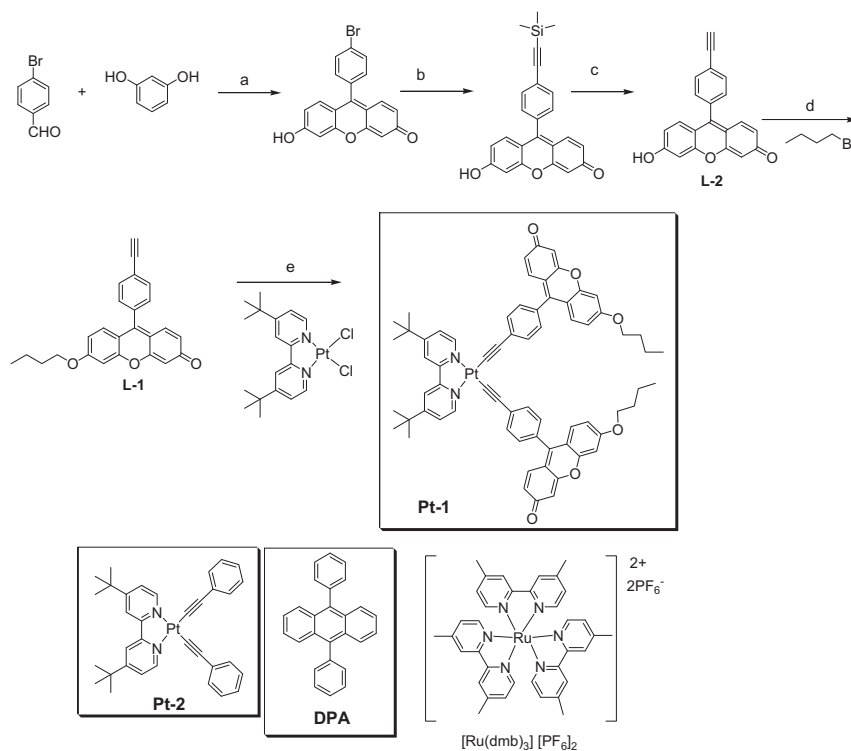
carboxylic moiety (**L-1**, Scheme 1). 8-Bromobenzenealdehyde and *m*-dihydroxybenzene were used as the starting materials. Acid catalyzed condensation of the two compounds produces the intermediate 9-(4-bromo)-6-hydroxy-3-fluorone. Then the acetylide bond was introduced by the Pd(0) catalyzed Sonogashira coupling reaction. We found that protection of the free hydroxyl moiety is necessary, otherwise the later metallation of the acetylide ligands will become troublesome. Thus the butylether **L-1** was prepared and was used for preparation of the complex **Pt-1**. **Pt-1** was obtained in satisfying yield.

2.2. Steady state photophysical properties

The UV–vis absorption of the complexes were studied (Fig. 1). The model complex **Pt-2** gives weak absorption in the visible region, $\epsilon = 8800 \text{ M}^{-1} \text{ cm}^{-1}$ at 424 nm. In comparison, **Pt-1** shows much stronger absorption, with $\epsilon = 24,600 \text{ M}^{-1} \text{ cm}^{-1}$ at 457 nm. Enhanced absorption in the visible region is beneficial for applications such as photocatalysis, photovoltaics, etc. Furthermore, we found that UV–vis absorption of **Pt-1** is roughly the sum of the ligand **L-1** and the model complex **Pt-2**, thus we propose that there is no strong electronic communication between the Pt(II) centre and the fluorescein chromophore core in **Pt-1**. This observation is weaker than the rhodamine-containing Pt(II) acetylide complex [20].

The emission of the ligands and the complexes were also studied (Fig. 2). **Pt-1** gives slightly red-shifted emission than the model complex **Pt-2** and the ligands (with toluene as solvent). All the emission bands are broad and structureless. We noted that the emission of **Pt-1** in ethanol is blue-shifted compared to that in toluene (see Supplementary data). The emission of **Pt-1** in ethanol is close to the emission of the ligand **L-1**.

The luminescence lifetimes (τ_L) of the compounds were measured. **Pt-1** gives τ_L value of 0.45 ns, which is much shorter than that of **Pt-2** (1.36 μs). **Pt-2** is known to show phosphorescence at RT.



Scheme 1. Synthesis and molecular structures of **L-1** and **Pt-1**. The triplet acceptor 9,10-diphenylanthracene (DPA) and the model complex $[\text{Ru}(\text{dmb})_3][\text{PF}_6]_2$ were also shown. (a) Methanesulfonic acid, 80 °C, 24 h. (b) (Trimethylsilyl) acetylene, CuI, $\text{PdCl}_2(\text{PPh}_3)_2$, PPh_3 , $\text{Et}_3\text{N}/\text{THF}$, Ar, 70 °C, 8 h. (c) K_2CO_3 , $\text{MeOH}/\text{CH}_2\text{Cl}_2$, r.t., 3 h. (d) K_2CO_3 , DMF, Ar, 60 °C, 8 h. (e) Diethylamine/ CH_2Cl_2 , CuI, Ar, r.t., 3 h.

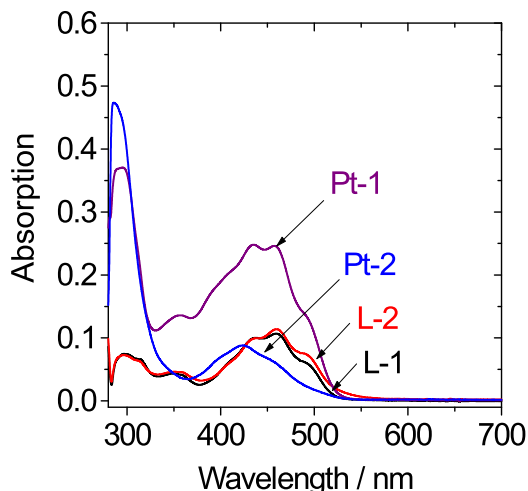


Fig. 1. UV–vis absorption of **Pt-1**, **Pt-2**, **L-1** and **L-2**, $c = 1.0 \times 10^{-5}$ M in toluene, 20 °C.

We tentatively attribute the emission of **Pt-1** to the fluorescence of the ligand, based on the emission wavelength and the lifetime.

The luminescence lifetime of **Pt-1** is shorter than the ligand **L-1** ($\tau = 1.87$ ns). This is due to the intramolecular energy transfer of $^1\text{IL} \rightarrow ^1\text{MLCT}$ state, or the intersystem crossing (ISC) $^1\text{IL} \rightarrow ^3\text{IL}$. However, these spectroscopic data are insufficient to be used for elucidation of the feature of emissive excited state of **Pt-1** as fluorescence or phosphorescence.

In order to assign the emission of **Pt-1**, the emission under different atmosphere of N_2 , air and O_2 were studied (Fig. 3a). We found that the emission intensity is independent on O_2 , i.e. the emission was not quenched by O_2 . This is an unambiguous indication of fluorescence for the emission of **Pt-1** [21]. By comparison with the emission of the ligands, the RT emission of **Pt-1** (Fig. 2) can be assigned as fluorescence of the fluorescein ligand. On the contrary, the emission of **Pt-2** is sensitive to O_2 , i.e. the emission was remarkably quenched by O_2 , which is an indication of phosphorescence [21].

2.3. 77 K Emission spectra

In order to study the possible intraligand ^3IL phosphorescence of the fluorescein, the emission spectra of **Pt-1** and **Pt-2** at 77 K were studied (Fig. 4). Compared to the emission at RT, the emission of **Pt-**

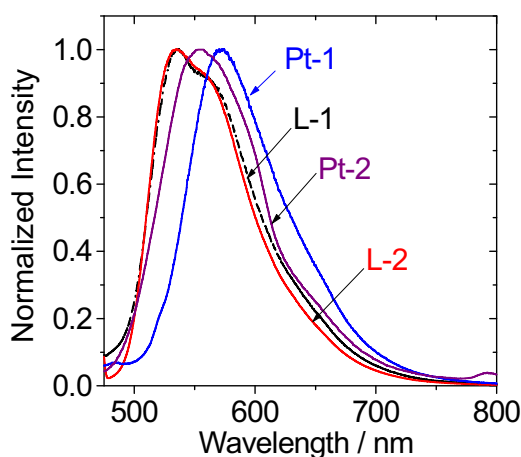


Fig. 2. The normalized emission of **Pt-1**, **Pt-2**, **L-1** and **L-2**, $c = 1.0 \times 10^{-5}$ M in toluene, 20 °C.

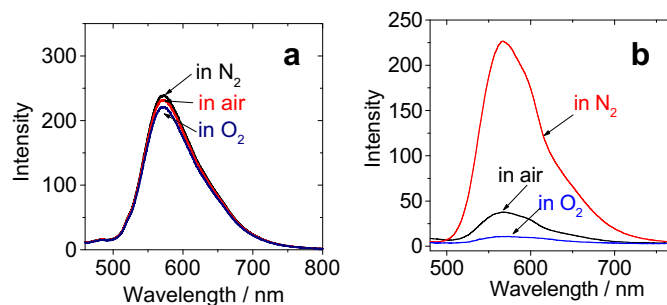


Fig. 3. Emission spectra of (a) **Pt-1** in EtOH and (b) **Pt-2** in toluene saturated with air, O_2 and N_2 , $c = 1.0 \times 10^{-5}$ M, 25 °C.

1 at 77 K shows new bands at 518 nm and 667 nm. This emission band at 667 nm was assigned to the phosphorescence of the fluorescein ligand, which is supported by the calculated T_1 state energy level of the ligand (1.67 eV, 742 nm). Observation of the phosphorescence at 77 K is reasonable since most of the non-radiative decay channel of the ^3IL excited state will be inhibited at 77 K, in solid matrix [34]. Previously rhodamine acetylide was attached to the Pt(II) centre, but the phosphorescence of rhodamine was not observed at 77 K [20].

The emission of **Pt-2** at 77 K was also measured (Fig. 4b). Compared to the RT emission, the emission at 77 K was blue-shifted to 499 nm and the emission band becomes more structured. The thermally induce Stokes shift is 2887 cm^{-1} . This large value is an indication of $^3\text{MLCT}$ emission for **Pt-2** [15–17,19,23,35].

It should be pointed out that the coordination centre of **Pt-1** is similar to that of **Pt-2**. In **Pt-1** the fluorescein core is electronically isolated from the Pt(II) centre by the phenyl moieties, which is confirmed by the UV–vis absorption of the complex (Fig. 1). However, the emission of **Pt-1** at 77 K (667 nm and 732 nm) is drastically different from that of **Pt-2**, thus, this result indicates that the near-IR emission of **Pt-1** is due to the ^3IL state (localized on the fluorescein moiety), not the $^3\text{MLCT}$ state. Some organic chromophore-containing complexes have been reported [8b,20,28], with the π -core of the chromophore not be directly connected to the metal centre. These complexes usually do not show the RT phosphorescence of the organic chromophore, due to the relatively weak ISC effect [20,36,37] Table 1.

2.4. Spin density analysis of the complex: assignment of the ^3IL excited state

Our anticipation of the population of the fluorescein-localized ^3IL excited state for **Pt-1** was supported by spin density analysis of the triplet state of the complex (Fig. 5) [14–20,38]. For the model

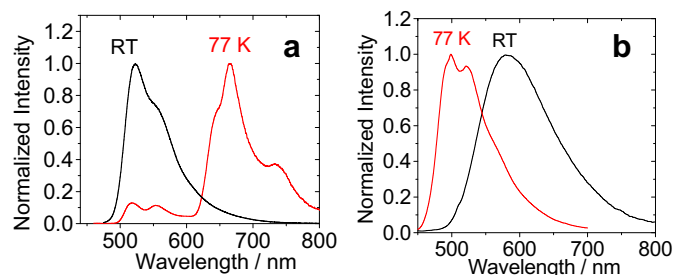


Fig. 4. Photoluminescence spectra of (a) **Pt-1** ($\lambda_{\text{ex}} = 442$ nm), (b) **Pt-2** ($\lambda_{\text{ex}} = 442$ nm) at RT and 77 K (EtOH:MeOH, 4:1, v/v).

Table 1
Photophysical parameters of Pt(II) complexes and the ligands.

	λ_{abs} (nm) ^a	λ_{em} (nm)	Φ_{F} ^b	τ^{c}	$k_{\text{r}}/s^{-1\text{d}}$	$k_{\text{nr}}/s^{-1\text{e}}$
L-1	440 (1.00), 460 (1.14)	534	0.86%	1.87 ns	4.60×10^6	5.30×10^8
L-2	437 (1.00), 353 (1.07)	532	1.14%	1.25 ns	9.12×10^8	6.33×10^8
Pt-1	435 (2.48), 457 (2.46)	570	0.66%	0.45 ns	1.47×10^7	2.21×10^9
Pt-2	424 (0.88)	567	42.2%	1.27 μs	3.32×10^5	4.55×10^5

^a Extinction coefficients ($10^4 \text{ M}^{-1} \text{ cm}^{-1}$) are shown in parentheses.

^b Fluorescence quantum yield with quinine sulphate as the standard ($\Phi_{\text{F}} = 0.547$ in 0.05 M sulphuric acid) in toluene.

^c Fluorescence lifetimes. Measured with luminescence method.

^d Radiative deactivation rate constant (k_{r}).

^e Non-radiative deactivation rate constant (k_{nr}). $k_{\text{r}} = \Phi_{\text{em}}/\tau_{\text{em}}$; $k_{\text{nr}} = (1/\tau_{\text{em}})(1 - \Phi_{\text{em}})$.

complex **Pt-2**, it is known that the lowest-lying triplet excited state is in ${}^3\text{MLCT}/{}^3\text{LLCT}$ (acetylide \rightarrow *dbbpy*) mixed feature [23]. The phenylacetylide, Pt(II) centre and the *dbbpy* moieties are all involved in the T_1 excited state of **Pt-2**. The spin density surface of **Pt-2** is distributed over the entire molecular framework, which is in full agreement with the ${}^3\text{MLCT}/{}^3\text{LLCT}$ excited state of **Pt-2** (Fig. 5).

For **Pt-1**, however, the spin density surface of the triplet state is located on the fluorescein moiety, the contribution of the Pt(II) atom is very small and the *dbbpy* ligand does not contribute to the spin density (Fig. 5). Thus, the lowest-lying triplet excited state of **Pt-1** can be described as a fluorescein-localized ${}^3\text{IL}$ excited state [14–20,38]. Furthermore, the minor involvement of the Pt(II) in the ${}^3\text{IL}$ state may be responsible for the lack of phosphorescence of **Pt-1** at RT, due to the weak heavy atom effect. Recently we observed similar results with the Pt(II) complexes that contain rhodamine moiety [20].

2.5. Nanosecond time-resolved transient difference absorption spectra

In order to prove the fluorescein-localized ${}^3\text{IL}$ excited state for **Pt-1**, the nanosecond time-resolved transient difference absorption spectra of **Pt-1** were studied (Fig. 6). Significant bleaching was found in the region 400–500 nm upon pulsed laser excitation. This bleaching is due to the depletion of the ground state of the fluorescein ligand, which shows strong steady state absorption at 450 nm (Fig. 1). Furthermore, transient absorption in the region of 500–800 nm was observed for **Pt-1** upon pulsed laser excitation. These features are drastically different from the time-resolved transient difference absorption spectra of **Pt-2** [37].

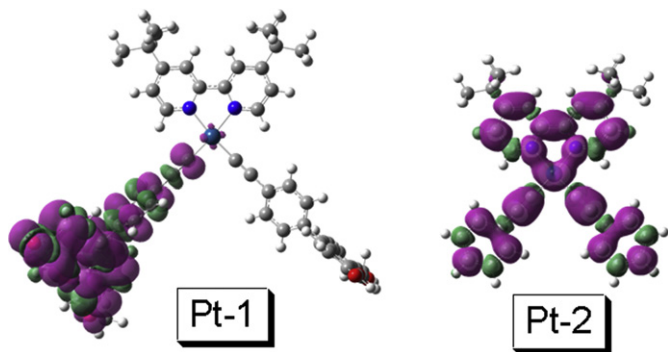


Fig. 5. Spin density surfaces of **Pt-1** and **Pt-2**. Solvent EtOH was considered in the calculation (PCM model). The calculations are based at the optimized triplet state geometry (isovalue: ± 0.0004). Calculated at B3LYP/6-31G/LANL2DZ level with Gaussian 09 W.

The calculations predict transient absorptions at 500–700 nm (Fig. 6b), which is in good agreement with the experimental results (Fig. 6a). Transient absorption at 530 nm, 620 nm and 660 nm were observed. These transient absorptions can be fully rationalized by TDDFT calculations on the transitions between the triplet excited states, such as $T_1 \rightarrow T_2$, etc. The calculations predict absorption bands of the T_1 state for **Pt-1** at 468 nm ($f = 0.2941$, $T_1 \rightarrow T_{24}$), 530 nm ($f = 0.0552$, $T_1 \rightarrow T_{18}$), 629 nm ($f = 0.0473$, $T_1 \rightarrow T_{12}$) and 662 nm ($f = 0.0332$, $T_1 \rightarrow T_{10}$). The intensive absorption of the T_1 state at 468 nm may be responsible for the decreased bleaching of ground state at ca. 460 nm.

Thus the transient difference absorption spectra supports the assignment of the triplet excited state of **Pt-1** as fluorescein-localized ${}^3\text{IL}$ excited state [20]. By following the decay of the transients at 530 nm, a lifetime of 16.4 μs was observed. This T_1 excited state lifetime is shorter than the rhodamine acetylide-containing Pt(II) complex (83.0 μs) [20]. However, the triplet excited state lifetime of **Pt-1** is still much longer than the usual N^*N Pt(II) bisacetylide complexes, usually shorter than 5 μs [23]. The T_1 state lifetime of **Pt-1** is longer than the PDI acetylide containing Pt(II) complex (0.246 μs) [28]. Transient metal complexes with long-lived T_1 excited states are beneficial for applications of these complexes in luminescent O_2 sensing [15,39–42], photocatalysis [43], and more recently TTA upconversions [8,13,15,19,20].

2.6. Energy level diagram of **Pt-1**

The photophysics of **Pt-1** can be summarized in Scheme 2. With excitation into the ${}^1\text{IL}$ state of **Pt-1**, i.e. the singlet excited state localized on the fluorescein ligand, the non-efficient ISC to ${}^3\text{IL}$ will lead to fluorescence of the ligand (${}^1\text{IL}^* \rightarrow \text{S}_0$) (Fig. 2). ${}^3\text{IL}$ is non-emissive due to the minor involvement of the Pt(II) centre, demonstrated by the molecular structure (the π -conjugation core is not directly attached to the Pt(II) centre) and the spin density analysis (Fig. 5). However, the long-lived ${}^3\text{IL}^*$ excited state can be detected with the time-resolved transient difference absorption spectroscopy (Fig. 6).

The **Pt-1** can also be excited with excitation into the MLCT band of the UV–vis absorption 380–450 nm (Fig. 1). In this case a fast ISC will lead to the efficient population of the ${}^3\text{MLCT}$ excited state, very often the efficiency is believed to be close to unity [8], although an energy transfer to the ${}^1\text{IL}$ can't be completely excluded. However, in both pathways the ${}^3\text{IL}^*$ excited state will be populated, for example, via internal conversion (IC) ${}^3\text{MLCT} \rightarrow {}^3\text{IL}$, because the energy level of the ${}^3\text{IL}$ state is lower than the ${}^3\text{MLCT}$ state. Thus the typical phosphorescence of the Pt(II) bisacetylide coordination centre at 499 nm was completely quenched in **Pt-1**.

We believe that **Pt-1** can be used for sensitizing some photo-physical processes even it is non-phosphorescent [12,18,20,44]. One of such applications is TTA based upconversion [7,8].

2.7. Application of the intense visible light absorption and long-lived T_1 excited state of **Pt-1** for TTA upconversion

Upconversion is important for photovoltaics, bioimaging and optics, etc [45,46]. Recently a new upconversion scheme has been developed, i.e. the TTA upconversion, which shows various advantages compared to the other upconversion techniques, such as two-photon absorption fluorescent dyes [25], or upconversion with rare earth metal materials [46], inorganic crystals (KDP crystals, etc) [47]. These tradition upconversions suffer from some disadvantages, such as requirement of coherent excitation light with high excitation power density (MW cm^{-2} , thus only pulsed laser is sufficient), low upconversion quantum yield, weak absorption of the excitation light, etc. With the TTA upconversion,

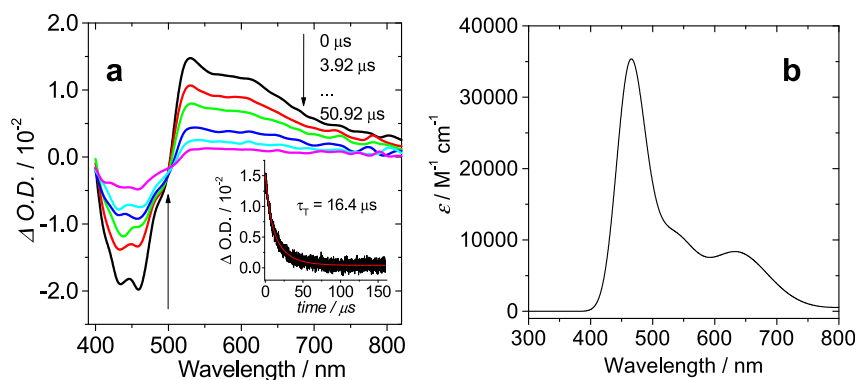
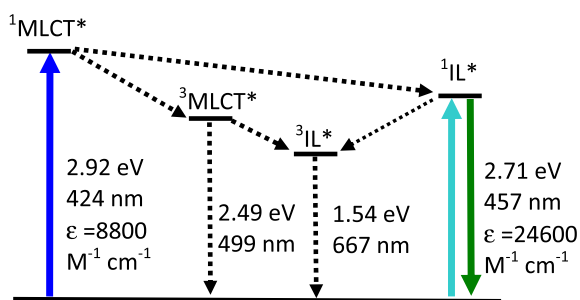


Fig. 6. (a) Transient absorption difference spectra of **Pt-1** in deaerated toluene after pulsed excitation ($\lambda_{\text{ex}} = 355$ nm). Inset: decay trace of **Pt-1** at 530 nm $[\text{Pt-1}] = 2.0 \times 10^{-5}$ M in toluene, 25 °C. (b) The calculated transient absorption spectra of the T_1 state of **Pt-1**. Please note that the information of bleaching is not included in the calculated transient absorption spectra. Based on the optimized triplet state geometry. EtOH was used as solvent in the calculations (PCM model). Calculated at B3LYP/6-31G(d)/LANL2DZ level with Gaussian 09 W.

however, all these disadvantages can be addressed [7–10]. For example, the TTA upconversion shows intense absorption of the excitation light, non-coherent excitation light with low excitation power density is sufficient for the upconversion, and the upconversion quantum yield is high [7,8,9,48].

TTA upconversion requires triplet sensitizer and triplet acceptor, and the compounds are mixed together for the upconversion [7,8]. With selective excitation of the triplet sensitizer, the energy is transferred to the triplet acceptor via triplet–triplet-energy-transfer (TTET), then two acceptor molecules at the triplet state will annihilate to produce an acceptor molecule at the singlet excited state. According to the spin statistical rule, the probability of producing of the singlet excited states in the annihilation product is 11.1% [7,8,49].

DPA was selected as the triplet acceptor for the TTA upconversion [7,8]. **Pt-2** was used as the model complex. Upon 473 nm CW laser irradiation, the sensitizers **Pt-1** or **Pt-2** give emission bands at 580 nm, and the emission of **Pt-2** is stronger than that of **Pt-1** (Fig. 7). Note the emission of **Pt-2** is phosphorescence but the emission of **Pt-1** is fluorescence. **Pt-1** is non-phosphorescent at RT. In the presence of DPA, the phosphorescence of **Pt-2** was quenched and weak upconverted emission at 415 nm was observed. For **Pt-1**, much more intense upconverted fluorescence of DPA was observed. It was known that DPA can not be excited with 473 nm laser, thus the emission for the **Pt-1**/DPA mixtures in the range of 400–500 nm is upconverted fluorescence of DPA. The upconversion quantum yield of the complexes **Pt-1** and **Pt-2** were determined as 10.7% and 4.4%, respectively. The TTA upconversion



Scheme 2. Quantitative Jablonski diagram for the photophysics of **Pt-1**. The excitation and the radiative decay from the excited state to the ground state are depicted by solid lines; whereas the non-radiative processes are illustrated by dotted lines. The energy levels of the $^3\text{MLCT}^*$ state and the $^3\text{IL}^*$ state are approximated as the emission of **Pt-2** and **Pt-1** at 77 K, respectively.

quantum yield of **Pt-1** is comparable to that with the rhodamine acetylide Pt(II) complex (11.2%) [20]. For the visible-light harvesting PDI-acetylide complex, however, we propose the TTA upconversion will be not significant, due to the short T_1 state lifetime of that complex [28].

Recently we propose that the upconversion capability of TTA upconversion can be described by $\eta = \epsilon \times \Phi_{\text{UC}}$, where ϵ is the molar extinction coefficient of the sensitizer at the excitation wavelength and Φ_{UC} is the upconversion quantum yield [8a]. For **Pt-1**, $\eta = 2018$ $\text{M}^{-1} \text{cm}^{-1}$, but for **Pt-2**, $\eta = 180$ $\text{M}^{-1} \text{cm}^{-1}$. Thus the upconversion capability of **Pt-1** is ca. 11-fold of that of **Pt-2**.

The upconversion with **Pt-1** as the triplet sensitizer is demonstrated by the visibility of the upconversion with un-aided eye (Fig. 8a). Blue emission was observed for the upconversion with **Pt-1**. For **Pt-2**, however, much weaker upconverted blue emission was observed. The emission colour changes of the solution were characterized by the CIE colour coordinates (Fig. 8b). The CIE coordinates of the emission of **Pt-1** and **Pt-2** alone are (0.43, 0.42) and (0.45, 0.46), respectively. In the presence of DPA, the CIE coordinates changed to (0.21, 0.13) and (0.43, 0.42), respectively. Thus the upconversion with **Pt-1** is more significant than that with **Pt-2**, and η value is a better criteria than Φ_{UC} value for the evaluation of the upconversion capability of a sensitizer, especially for applications such as photovoltaics and photocatalysis, etc.

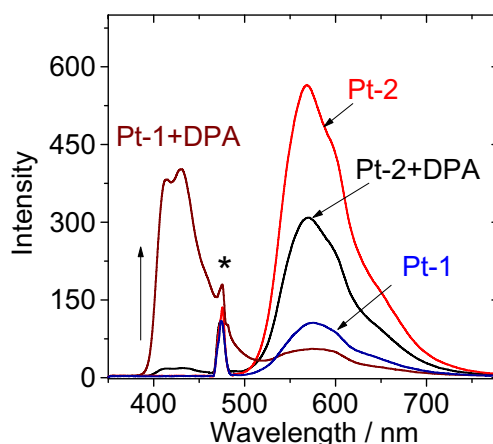


Fig. 7. Upconversion with **Pt-1** and **Pt-2** (1.0×10^{-5} M) as the triplet sensitizers. DPA (2.0×10^{-4} M) was used as the triplet acceptor. The emission of the sensitizers alone were also presented. Excited with 473 nm laser (5 mW). In toluene, 25 °C. The asterisks indicate the scattered 473 nm laser.

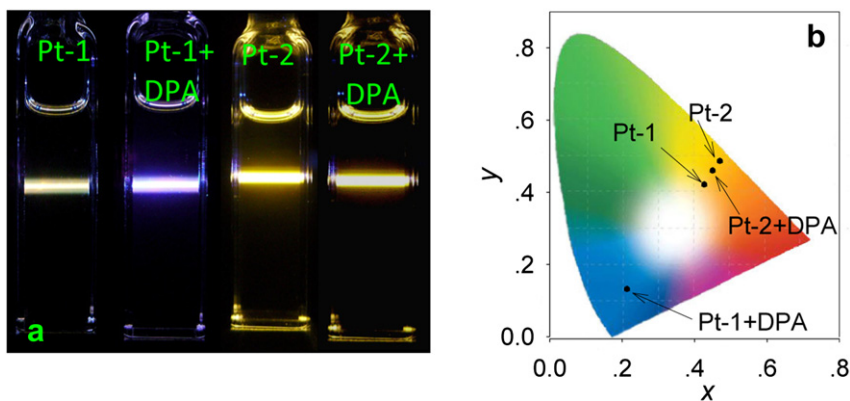


Fig. 8. (a) Photographs of upconversions with **Pt-1** and **Pt-2** as the triplet sensitizers and 9,10-diphenylanthracene (DPA) as the triplet acceptor. Photographs of the phosphorescence and the upconversion of the complexes. Excitation by blue laser ($\lambda_{\text{ex}} = 473 \text{ nm}$, 5 mW). 20 °C. (b) The CIE coordinate changes of triplet sensitizers before and after adding 9,10-diphenylanthracene (DPA). (For interpretation of the references to colour in this figure legend, the reader is referred to the web version of this article.)

The process of TTA upconversion can be summarized in Scheme 3 [7,8]. Based on the Jablonski diagram, the TTET process is important for the TTA upconversion. Accordingly, two parameters of the triplet sensitizer are crucial for the TTA upconversion. One is the absorption of the excitation light and another is the lifetime of the T_1 excited state of the triplet sensitizer. Either high concentration of the triplet sensitizer (as a result of the intense absorption of the excitation light by the sensitizer) at the T_1 excited state or the long-lived T_1 excited state will enhance the TTET process, with which the TTA upconversion can be improved. The intense absorption of visible light and the long-lived T_1 excited state of **Pt-1** make it an ideal candidate as the triplet sensitizer for TTA upconversion. Furthermore, it should be pointed out that the triplet state involved in the TTET process is non-emissive. Most of the triplet sensitizers for TTA upconversion are phosphorescent [7,8], except very few examples [12,14,18]. Application of non-phosphorescent transition metal complexes as triplet sensitizers for TTA upconversion will greatly increase the availability of the triplet sensitizers for TTA upconversion (please note that the triplet excited state of the sensitizer must be populated upon photoexcitation), and other appropriate photophysical processes.

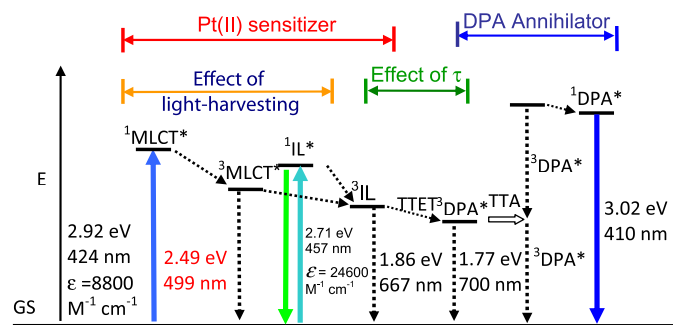
3. Conclusions

Fluorescein-containing N^*N Pt(II) bisacetylde complex (**Pt-1**) was prepared (where $N^*N = 3,3'$ -di-*t*-butyl-2,2'-bipyridine, *dbbpy*). The fluorescein moiety was connected to the Pt(II) centre via acetylde bond at the 4-position of the phenyl group of the fluorescein. **Pt-1** shows strong absorption of visible light ($\epsilon = 24,600 \text{ M}^{-1} \text{ cm}^{-1}$ at 457 nm). Fluorescence of the ligand was observed for **Pt-1** at room temperature ($\tau = 0.45 \text{ ns}$). At 77 K, a phosphorescence band at 667 nm was observed. Spin density analysis of the triplet state and the nanosecond time-resolved transient difference absorption spectroscopy indicated that the lowest-lying triplet excited state of the complex is the fluorescein-localized intraligand triplet excited (^3IL state), for which the lifetime was determined as 16.4 μs by nanosecond time-resolved transient difference absorption spectroscopy. This lifetime is much longer than the lifetime of the T_1 excited state of ordinary Pt(II) bisacetylde complexes (less than 5 μs). The lack of the normal MLCT phosphorescence of **Pt-1** is attributed to the internal conversion from the $^3\text{MLCT}$ excited state to the ^3IL excited state, due to the much lower energy level of the ^3IL state than the $^3\text{MLCT}$ state. The complex **Pt-1** was used as the triplet sensitizer for triplet-triplet annihilation upconversion, for which the quantum yield is 10.7%. For the model complex (**Pt-2**) without the fluorescein moiety, the upconversion quantum yield is 4.4%. The overall upconversion performance of **Pt-1** (η) is 11-fold of **Pt-2**. We proved that the complex with intense absorption of visible light and long-lived triplet excited state can be accessed with the Pt(II) complex in which an organic chromophore is attached to the transition metal atom. These transition metal complexes are beneficial for the applications in the triplet-triplet-energy-transfer, which is crucial for a variety of photophysical processes, such as photodynamic therapy (PDT) or TTA upconversions, etc.

4. Experimental section

4.1. General information

NMR spectra were recorded on a 400 MHz Varian Unity Inova NMR spectrophotometer. Mass spectra were recorded with Q-TOF Micro MS spectrometer. UV-vis absorption spectra were measured with a HP8453 UV-visible spectrophotometer. Fluorescence spectra were recorded on a Shimadzu RF5301PC spectrofluorometer or a Sanco 970 CRT spectrofluorometer. Fluorescence quantum yields were measured with reference quinine sulphate ($\Phi = 54.7\%$



Scheme 3. Qualitative Jablonski Diagram illustrating the sensitized TTA up conversion process between Pt(II) complexes (exemplified by **Pt-1**) and DPA. The effect of the light-harvesting ability and the luminescence lifetime of the Pt(II) sensitizer on the efficiency of the TTA upconversion is also shown. E is energy. GS is ground state (S_0). $^1\text{IL}^*$ is intraligand singlet excited state (fluorescein localized). IC is internal conversion. ISC is intersystem crossing. $^3\text{MLCT}^*$ is the Pt(II) based metal-to-ligand-charge-transfer triplet excited state. $^3\text{IL}^*$ is intraligand triplet excited state (fluorescein localized). TTET is triplet-triplet energy transfer. $^3\text{DPA}^*$ is the triplet excited state of DPA. TTA is triplet-triplet annihilation. $^1\text{DPA}^*$ is the singlet excited state of DPA. The emission bands observed for the sensitizers alone is the $^1\text{IL}^*$ emissive excited state. The emission bands observed in the TTA upconversion experiment is the simultaneous $^1\text{IL}^*$ emission (fluorescence) and the $^1\text{DPA}^*$ emission (fluorescence).

in 0.05 M sulphuric acid). Luminescence lifetimes were measured on an OB920 phosphorescence/fluorescence lifetime spectrometer (Time resolution is 100 ps. Edinburgh Instruments, U.K.).

4.2. Synthesis

4.2.1. 9-(4-Bromophenyl)-6-hydroxy-3-fluorone

4-Bromobenzaldehyde (1.85 g, 10 mmol) and *m*-dihydroxybenzene (2.20 g, 20 mmol) was dissolved in methanesulfonic acid (25 mL). The solution was stirred at 80 °C for 24 h. After cooled to r.t., the reaction mixture was poured into 200 mL NaOAc solution (3 M). Black precipitate was collected and washed with water (3 × 50 mL). After drying in vacuum, the precipitate was purified by column chromatography (silica gel, CH₂Cl₂/MeOH = 10:1, v/v) for twice. 0.53 g dark red solid was obtained. Yield: 14.4%. ¹H NMR (400 MHz, CDCl₃/CD₃OD): δ 7.77 (d, *J* = 8.8 Hz, 2H), 7.29 (d, *J* = 8.0 Hz, 2H), 7.22 (d, *J* = 9.2 Hz, 2H), 6.78–7.76 (m, 4H). TOF MS EI: calcd for C₁₉H₁₁O₃Br [M]⁺ *m/z* = 365.9892, found *m/z* = 365.9904.

4.2.2. L-2

(Trimethylsilyl) acetylene (0.33 mL, 2.32 mmol) and CuI (5.7 mg, 0.03 mmol) were added to a degassed solution of 9-(4-bromophenyl)-6-hydroxy-3-fluorone (0.35 g, 1.00 mmol), PdCl₂(PPh₃)₂ (21.2 mg, 0.03 mmol), PPh₃ (15.7 mg, 0.06 mmol) in triethylamine (15 mL) and THF (20 mL). The reaction mixture was heated at 70 °C for 8 h. Then the mixture was evaporated to dryness and the crude product was purified by column chromatography (silica gel, CH₂Cl₂/MeOH = 10:1, v/v) twice. A red solid was obtained (the trimethylsilyl protected acetylide). K₂CO₃ (414.0 mg, 3.00 mmol) was added to a methanol (5 mL) and CH₂Cl₂ solution (5 mL) of the red solid obtained above and the mixture was stirred at room temperature for 3 h. The solvent was evaporated and water (10 mL) was added. Then the mixture was extracted with CH₂Cl₂. The organic layer was dried and then the crude product was purified by column chromatography (silica gel, CH₂Cl₂/MeOH = 10:1, v/v) twice. A red solid was obtained; yield 170.0 mg, 0.54 mmol, 54.5%. ¹H NMR (400 MHz, CDCl₃/CD₃OD): δ 7.74 (d, *J* = 7.2 Hz, 2H), 7.39 (d, *J* = 7.2 Hz, 2H), 7.27 (d, *J* = 8.8 Hz, 2H), 6.81–6.90 (m, 4H), 3.41 (s, 1H). ¹³C NMR (100 MHz, CDCl₃ + CD₃OD) 158.0, 155.0, 132.3, 131.4, 129.4, 124.3, 121.5, 115.1, 103.5, 82.2, 79.7. TOF MS ES: calcd for C₂₁H₁₁O₃ ([M – H][−]) *m/z* = 311.0708, found *m/z* = 310.9245.

4.2.3. L-1

L-2 (150.0 mg, 0.48 mmol) and K₂CO₃ (198.9 mg, 1.44 mmol) was dissolved in 2 mL DMF under nitrogen and heated to 60 °C. Then, 1-bromobutane (198.0 mg, 1.44 mmol) was added to the mixture dropwise, and the mixture was heated at 60 °C for 8 h. The reaction mixture was poured into ice water (100 mL). Red precipitate was collected and washed with water (3 × 50 mL). After drying under vacuum, the precipitate was purified by column chromatography (silica gel, CH₂Cl₂/MeOH = 30:1, v/v) twice. A dark red solid was obtained; yield: 60.0 mg (0.16 mmol), 33.3%. ¹H NMR (400 MHz, CDCl₃): δ 7.69 (d, *J* = 8.0 Hz, 2H), 7.32 (d, *J* = 8.0 Hz, 2H), 7.06–7.12 (m, 2H), 6.93 (s, 1H), 6.76 (d, *J* = 12.0 Hz, 1H), 6.58 (d, *J* = 8.0 Hz, 1H), 6.46 (s, 1H), 4.09 (t, *J* = 8.0 Hz, 2H), 3.22 (s, 1H), 1.81–1.84 (m, 2H), 1.49–1.54 (2H), 1.00 (t, *J* = 8.0 Hz, 3H). ¹³C NMR (100 MHz, CDCl₃) δ 185.5, 164.0, 158.8, 154.7, 148.4, 133.4, 132.4, 130.5, 130.1, 129.5, 129.4, 123.6, 117.9, 114.0, 113.8, 106.0, 100.8, 82.6, 79.1, 68.7, 30.9, 19.1, 13.7. TOF MS ES: calcd for C₂₅H₂₀O₃Na ([M + Na]⁺) *m/z* = 391.1310, found *m/z* = 391.1887.

4.2.4. Pt-1

Pt(*dbbpy*)Cl₂ (12.8 mg, 0.02 mmol), L-2 (22.0 mg, 0.06 mmol), and diethylamine (0.2 mL) were dissolved in CH₂Cl₂ (3 mL). The

mixture was purged with Ar for 20 min, then CuI (2.5 mg, 0.05 mmol) was added under Ar, and the mixture was stirred at room temperature for 3 h. The reaction mixture was purified by column chromatography (silica gel, CH₂Cl₂/CH₃OH = 30:1, v/v). A red solid was obtained (22.1 mg), yield 92.2%. ¹H NMR (400 MHz, CDCl₃): δ 9.71 (d, *J* = 8.0 Hz, 2H), 8.01 (s, 2H), 7.72 (d, *J* = 8.0 Hz, 4H), 7.65 (d, *J* = 4.0 Hz, 2H), 7.23–7.29 (m, 8H), 6.93 (s, 2H), 6.78 (d, *J* = 12.0 Hz, 2H), 6.61 (d, *J* = 8.0 Hz, 2H), 6.47 (s, 2H), 4.09 (t, *J* = 8.0 Hz, 4H), 1.81–1.85 (m, 4H), 1.45–1.57 (m, 2H), 1.00 (t, *J* = 8.0 Hz, 6H). ¹³C NMR (100 MHz, CDCl₃) δ 163.8, 156.1, 154.7, 151.1, 132.1, 131.0, 129.9, 129.5, 129.0, 118.8, 117.6, 114.3, 113.6, 105.6, 100.6, 68.6, 35.8, 30.9, 30.2, 19.1, 13.7. MALDI-HRMS: calcd for C₆₈H₆₃N₂O₆Pt ([M + H]⁺) *m/z* = 1198.4334, found *m/z* = 1198.4250.

4.3. Nanosecond time-resolved transient difference absorption spectroscopy

The nanosecond time-resolved transient difference absorption spectra were recorded on LP 920 laser flash photolysis spectrometer (Edinburgh Instruments, UK). The samples were purged with N₂ or Ar for 15 min before measurements. The samples were excited with 355 nm pulsed laser and the transient signals were recorded on a Tektronix TDS 3012B oscilloscope. The data were analyzed by LP900 software.

4.4. Computational methods

The geometry optimizations were calculated using B3LYP functional at 6-31G(d)/LanL2DZ level. The energy of the triplet excited state of the ligand was calculated with the time-dependent DFT (TDDFT) method based on the optimized singlet ground state geometry. The spin-density was calculated with the energy minimized triplet state geometries. All calculations were performed using Gaussian 09 W (Gaussian, Inc.) [50].

4.5. Upconversions

Pumped solid state laser was used as the excitation source for the upconversions. The samples were purged with N₂ or Ar for 15 min before measurement. The upconversion quantum yields were determined with the phosphorescence of Ru(dmb)₃[PF₆]₂ as the quantum yield standard ($\Phi = 0.074$ in MeCN) and the quantum yields were calculated with Eq. (1), where U_{unk} , A_{unk} , I_{unk} and η_{unk} represent the quantum yield, absorbance, integrated photoluminescence intensity, and the refractive index of the solvents, respectively. The photography of the upconversion were taken with Samsung NV5 digital camera. The exposure times are the default values of the camera.

$$\Phi_{\text{UC}} = 2\Phi_{\text{std}} \left(\frac{A_{\text{std}}}{A_{\text{unk}}} \right) \left(\frac{I_{\text{unk}}}{I_{\text{std}}} \right) \left(\frac{\eta_{\text{unk}}}{\eta_{\text{std}}} \right)^2 \quad (1)$$

Acknowledgements

We thank the NSFC (20972024 and 21073028), the Fundamental Research Funds for the Central Universities (DUT10ZD212), Ministry of Education (SRFDP-200801410004 and NCET-08-0077), the Royal Society (UK) and NSFC (China-UK Cost-Share Science Networks, 21011130154) for financial support.

Appendix A. Supplementary data

Supplementary data associated with this article can be found, in the online version, at doi:10.1016/j.jorganchem.2012.05.010.

References

- [1] T. Hirano, K. Kikuchi, Y. Urano, T. Higuchi, T. Nagano, *J. Am. Chem. Soc.* 122 (2000) 12399–12400.
- [2] H. Kojima, N. Nakatsubo, K. Kikutci, S. Kawahara, Y. Kirino, H. Nagoshi, Y. Hirata, T. Nagano, *Anal. Chem.* 70 (1998) 2446–2453.
- [3] H. Maeda, H. Matsuno, M. Ushida, K. Katayama, K. Saeki, N. Itoh, *Angew. Chem. Int. Ed.* 44 (2005) 2922–2925.
- [4] H. Maeda, K. Katayama, H. Matsuno, T. Uno, *Angew. Chem. Int. Ed.* 45 (2006) 1810–1813.
- [5] S.H. Lim, C. Thivierge, P. Nowak-Sliwinska, J. Han, H. van den Bergh, G. Wagnières, K. Burgess, H.B. Lee, *J. Med. Chem.* 53 (2010) 2865–2874.
- [6] S. Takizawa, R. Aboshi, S. Murata, *Photochem. Photobiol. Sci.* 10 (2011) 895–903.
- [7] T.N. Singh-Rachford, F.N. Castellano, *Coord. Chem. Rev.* 254 (2010) 2560–2573.
- [8] (a) J. Zhao, S. Ji, H. Guo, *RSC Adv.* 1 (2011) 937–950;
(b) J. Zhao, S. Ji, W. Wu, W. Wu, H. Guo, J. Sun, H. Sun, Y. Liu, Q. Li, L. Huang, *RSC Adv.* 2 (2011) 1712–1728.
- [9] A. Monguzzi, J. Mezyk, F. Scotognella, R. Tubino, F. Meinardi, *Phys. Rev. B* 78 (2008) 195112–1.
- [10] Y.Y. Cheng, T. Khoury, R.G.C.R. Clady, M.J.Y. Tayebjee, N.J. Ekins-Daukes, M.J. Crossley, T.W. Schmidt, *Phys. Chem. Chem. Phys.* 12 (2010) 66–71.
- [11] T.N. Singh-Rachford, R.R. Islangulov, F.N. Castellano, *J. Phys. Chem. A* 112 (2008) 3906–3910.
- [12] H. Chen, C. Hung, K. Wang, H. Chen, W.S. Fann, F. Chien, P. Chen, T.J. Chow, C. Hsu, S. Sun, *Chem. Commun.* (2009) 4064–4066.
- [13] S. Ji, W. Wu, W. Wu, H. Guo, J. Zhao, *Angew. Chem. Int. Ed.* 50 (2011) 1626–1629.
- [14] S. Ji, H. Guo, W. Wu, W. Wu, J. Zhao, *Angew. Chem. Int. Ed.* 50 (2011) 8283–8286.
- [15] W. Wu, W. Wu, S. Ji, H. Guo, J. Zhao, *Dalton Trans.* 40 (2011) 5953–5963.
- [16] H. Sun, H. Guo, W. Wu, X. Liu, J. Zhao, *Dalton Trans.* 40 (2011) 7834–7841.
- [17] Y. Liu, W. Wu, J. Zhao, X. Zhang, H. Guo, *Dalton Trans.* 40 (2011) 9085–9089.
- [18] W. Wu, H. Guo, W. Wu, S. Ji, J. Zhao, *J. Org. Chem.* 76 (2011) 7056–7064.
- [19] J. Sun, W. Wu, H. Guo, J. Zhao, *Eur. J. Inorg. Chem.* (2011) 3165–3173.
- [20] L. Huang, L. Zeng, H. Guo, W. Wu, W. Wu, S. Ji, J. Zhao, *Eur. J. Inorg. Chem.* (2011) 4527–4533.
- [21] J.R. Lakowicz, *Principles of Fluorescence Spectroscopy*, second ed. Lower Academic/Plenum Publishers, New York, 1999.
- [22] N.J. Turro, V. Ramamurthy, J.C. Scaiano, *Principles of Molecular Photochemistry: An Introduction*, University Science Books, Sausalito, CA, 2009.
- [23] J.A.G. Williams, *Top. Curr. Chem.* 281 (2007) 205–268.
- [24] N.D. McClenaghan, Y. Leydet, B. Maubert, M.T. Indelli, S. Campagna, *Coord. Chem. Rev.* 249 (2005) 1336–1350.
- [25] L. Flamigni, A. Barbieri, C. Sabatini, B. Ventura, F. Barigellet, *Top. Curr. Chem.* 281 (2007) 143–203.
- [26] W.Y. Wong, C.L. Ho, *Coord. Chem. Rev.* 253 (2009) 1709–1758.
- [27] (a) M. Hissler, W.B. Connick, D.K. Geiger, J.E. McGarrah, D. Lipa, R.J. Lachicotte, R. Eisenberg, *Inorg. Chem.* 39 (2000) 447–457;
(b) C.E. Whittle, J.A. Weinstein, M.W. George, K.S. Schanze, *Inorg. Chem.* 40 (2001) 4053–4062.
- [28] A.A. Rachford, S. Goeb, F.N. Castellano, *J. Am. Chem. Soc.* 130 (2008) 2766–2767.
- [29] F. Hua, S. Kinayyigit, A.A. Rachford, E.A. Shikhova, S. Goeb, J.R. Cable, C.J. Adams, K. Kirschbaum, A.A. Pinkerton, F.N. Castellano, *Inorg. Chem.* 46 (2007) 8771–8783.
- [30] P. Lane, J. Fallout, L. Toupee, J.A.G. Williams, H. Le Boozee, V. Guerschais, *Chem. Commun.* (2008) 4333–4335.
- [31] Y. Shao, Y. Yang, *Adv. Mater.* 17 (2005) 2841–2844.
- [32] F. Guo, Y.-G. Kim, J.R. Reynolds, K.S. Schanze, *Chem. Commun.* (2006) 1887–1889.
- [33] H. Guo, M.L. Muro-Small, S. Ji, J. Zhao, F.N. Castellano, *Inorg. Chem.* 49 (2010) 6802–6804.
- [34] F. Nastasi, F. Puntoriero, S. Campagna, S. Diring, R. Ziessel, *Phys. Chem. Chem. Phys.* 10 (2008) 3982–3986.
- [35] I.E. Pomestchenko, C.R. Luman, M. Hissler, R. Ziessel, F.N. Castellano, *Inorg. Chem.* 42 (2003) 1394–1396.
- [36] A.A. Rachford, R. Ziessel, T. Bura, P. Retailleau, F.N. Castellano, *Inorg. Chem.* 49 (2010) 3730–3736.
- [37] M. Galletta, F. Puntoriero, S. Campagna, C. Chiorboli, M. Quesada, S. Goeb, R. Ziessel, *J. Phys. Chem. A* 110 (2006) 4348–4358.
- [38] K. Hanson, A. Tamayo, V. V. Diev, M.T. Whited, P.I. Djurovich, M.E. Thompson, *Inorg. Chem.* 49 (2010) 6077–6084.
- [39] S. Ji, W. Wu, W. Wu, P. Song, K. Han, Z. Wang, S. Liu, H. Guo, J. Zhao, *J. Mater. Chem.* 20 (2010) 1953–1963.
- [40] W. Wu, W. Wu, S. Ji, H. Guo, P. Song, K. Han, L. Chi, J. Shao, J. Zhao, *J. Mater. Chem.* 20 (2010) 9775–9786.
- [41] H. Guo, S. Ji, W. Wu, W. Wu, J. Shao, J. Zhao, *Analyst* 135 (2010) 2832–2840.
- [42] W. Wu, W. Wu, S. Ji, H. Guo, Z. Zhao, *J. Organomet. Chem.* 696 (2011) 2388–2398.
- [43] X. Wang, S. Goeb, Z. Ji, N.A. Pogulaichenko, F.N. Castellano, *Inorg. Chem.* 50 (2011) 705–707.
- [44] T.N. Singh-Rachford, F.N. Castellano, *J. Phys. Chem. A* 113 (2009) 5912–5917.
- [45] C. Reinhard, R. Valiente, H.U. Gu1del, *J. Phys. Chem. B* 106 (2002) 10051–10057.
- [46] (a) M. Haase, H. Schäfer, *Angew. Chem. Int. Ed.* 50 (2011) 5808–5829;
(b) W. Wu, L. Yao, T. Yang, R. Yin, F. Li, Y. Yu, *J. Am. Chem. Soc.* 133 (2011) 15810–15813.
- [47] S.K. Kushwaha, M. Shakir, K.K. Maurya, A.L. Shah, M.A. Wahab, G. Bhagavannarayana, *J. Appl. Phys.* 108 (2010) 033506–1.
- [48] S. Balushev, V. Yakutkin, T. Miteva, Y. Avlasevich, S. Chernov, S. Aleshchenkov, G. Nelles, A. Cheprakov, A. Yasuda, K. Müllen, G. Wegner, *Angew. Chem. Int. Ed.* 46 (2007) 7693–7696.
- [49] J. Salties, G.R. Marchand, W.K. Smothers, S.A. Stout, J.L. Charlton, *J. Am. Chem. Soc.* 103 (1981) 7159–7164.
- [50] M.J. Frisch, G.W. Trucks, H.B. Schlegel, G.E. Scuseria, M.A. Robb, J.R. Cheeseman, G. Scalmani, V. Barone, B. Mennucci, G.A. Petersson, H. Nakatsuji, M. Caricato, X. Li, H.P. Hratchian, A.F. Izmaylov, J. Bloino, G. Zheng, J.L. Sonnenberg, M. Hada, M. Ehara, K. Oyota, R. Fukuda, J. Hasegawa, M. Ishida, T. Nakajima, Y. Honda, O. Kitao, H. Nakai, T. Vreven, J.A. Montgomery Jr., J.E. Peralta, F. Ogliaro, M. Bearpark, J.J. Heyd, E. Brothers, K.N. Kudin, V.N. Staroverov, R. Kobayashi, J. Normand, K. Raghavachari, A. Rendell, J.C. Burant, S.S. Iyengar, J. Tomasi, M. Cossi, N. Rega, N.J. Millam, M. Klene, J.E. Knox, J.B. Cross, V. Bakken, C. Adamo, J. Jaramillo, R. Gomperts, R.E. Stratmann, O. Yazyev, A.J. Austin, R. Cammi, C. Pomelli, J.W. Ochterski, R.L. Martin, K. Morokuma, V.G. Zakrzewski, G.A. Voth, P. Salvador, J.J. Dannenberg, S. Dapprich, A.D. Daniels, Ö. Farkas, J.B. Foresman, J.V. Ortiz, J. Cioslowski, D.J. Fox, *Gaussian 09 Revision A.1*, Gaussian Inc., Wallingford CT, 2009.